6

Low Temperature Crystal Structure of Rubrene Single Crystals Grown by Vapor Transport*

The study presented in the following chapter is promoted by reports of a precipitous drop in the electronic mobility of rubrene single crystals below 175 K. We assign this change to a phase transition. We perform the crystal structure determination for rubrene single crystals, $C_{42}H_{28}$ (5,6,11,12 - Tetraphenyltetracene), in the temperature interval 100 K - 300 K. The crystals are grown by physical vapor transport in an open system. The crystal structure is orthorhombic over the entire temperature range. We find evidence for a phase transition from Differential Scanning Calorimetry measurements, but see no evidence for a structural phase transition in the diffraction experiments.

*This Chapter is adapted from O. D. Jurchescu, A. Meetsma, and T. T. M. Palstra, Acta Cryst. B **62**, 330 (2006)

6.1 Introduction

The electronic properties of polymers and molecular crystals are of much current interest due to fundamental questions regarding electron transport and associated applications. The present focus is in developing novel chemical structures, as well as improved fabrication techniques that are able to open new fields for electronic applications based on organic materials.

A number of molecular conductors are of current interest. Rubrene (Fig. 6.1) exhibits interesting physical properties such as having one of the highest reported electronic mobilities at room temperature [1] (20 cm^2/Vs). Emerging new applications based on rubrene are organic field effect transistors (OFETs) [1–4] and organic light emitting diodes (OLEDs) [5, 6].

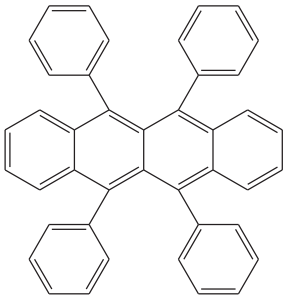

Figure 6.1: Bond-line formula of rubrene

.

Although the technological development is relatively fast, fundamental questions concerning the intrinsic mechanism of conduction have still not been answered. Moreover, for the title compound, little attention has been paid to the interplay between its crystal structure and electronic properties. The interest in the present work is guided by intriguing changes which have been observed at low temperature in the mobility of field-effect transistors built on rubrene single crystals [2, 3].

6.2 Polymorphism in rubrene

In this study, we investigate the structure of rubrene single crystals and correlate it with the electrical properties. The crystals are formed through competition

between π- stacking and quadrupolar interactions. Owing to these weak interactions, different growth conditions can lead to different polymorphs. This feature is widely encountered for molecular crystals. Several polymorphs of rubrene have been reported. A monoclinic phase was described by Taylor (1936) [7] and a triclinic polymorph was explored by Akopyan *et al.*(1962) [8]. Unfortunately, these reports do not mention the growth method. An orthorhombic form of rubrene (space group *Aba*2) was reported by Henn *et al.* (1971) [9] for crystals grown from vapor in vacuum using sealed ampoules. For crystals obtained in a closed system, in a two-zone furnace, at ambient pressure, Bulgarovskaya *et al.* (1983) reported a second orthorhombic polymorph, with space group *Bbam* [10]. For all the polymorphs investigated previously, only the room-temperature structure is reported, thus no relation with the physical properties at low temperature can be made.

6.3 Growth of rubrene single crystals

Rubrene single crystals investigated in this work were grown using physical vapor transport under a temperature gradient, in a horizontal tube [11]. The inner tube, in which the crystallization takes place, was cleaned and heated afterwards at $T = 600$ K under Ar flow for 10 hours to evaporate the solvents. The source material, with nominal 98% purity, was obtained from Sigma Aldrich. Prior to crystal growth, the powder was purified using vacuum sublimation under a temperature gradient process [12], designed to remove the light impurities[1]. The purified powder was placed in the hot part of the growth tube in a alumina boat. The sublimation temperature ($T = 553$ K) was kept as low as possible (close to the sublimation threshold). This was done to prevent the sublimation of heavy impurities and to ensure the slow sublimation rate that yields crystals with a minimum number of structural defects. Crystals grown at slightly higher temperatures were of significantly lower quality and gave weak diffraction pattern. The growth set-up was placed in dark to avoid oxidation. The transport gas was a mixture of H_2 (AGA, $5N$) and Ar (AGA, $5N$), with a volume percentage of 5.25% H_2.

The crystals are orange-colored and needle- or platelet-shaped. The typical in-plane dimensions are 200 μ m $\times 1$ cm for the needles and $3-5$ mm for platelets. The thickness of the crystals is $3-20$ μ m.

[1] We refer to the species present in the system that have lower/higher molecular masses than the parent compound as 'light'/'heavy' impurities.

6.4 Single crystal diffraction

6.4.1 Experimental details

The single crystal diffraction experiments were performed on a Bruker SMART APEX CCD diffractometer. A crystal fragment, cut to size to fit in the homogeneous part of the X-ray beam, with dimensions of 0.51 x 0.45 x 0.03 mm was mounted on top of a glass fiber and aligned on the diffractometer. The diffractometer was equipped with a 4K CCD detector set 60 mm from the crystal. Intensity measurements were performed using graphite monochromated Mo-$K_{\overline{\alpha}}$ radiation. The crystal was cooled fast using a Bruker KRYOFLEX (1h was taken to reach 100 K) and the measurements were performed during heating, after the temperature was stabilized. For each temperature investigated in this chapter, a total of 1800 frames were collected with an exposure time of 30.0 seconds per frame. The overall data collection time was 18.0 h. During this time, the variations in the temperature were ± 0.5 K at 100 K, and at most ± 2 K at higher temperatures.

The structure was solved by direct methods with SHELXS-97. The positional and anisotropic displacement parameters for the non-hydrogen atoms were refined.

Experimental details about the structure determination, data collection and refinement are summarized in the Appendix B of the thesis. The data collection (radiation type, monochromator, data collection method, θ range) and refinement parameters (number of reflections, number of refined parameters, weighting scheme, goodness of fit) are similar for the structures corresponding to the eight temperatures investigated in this study.

6.4.2 Orthorhombic rubrene

Crystals grown from physical vapor transport in an inert gas, in an open system and continuous flow [11] are preferred for electronic applications, because they present the highest purity and thus the largest mobility. Still, no crystal structure determination is available for crystals obtained by this method. In this study we report the crystal structure between 100 K and 300 K of rubrene single crystals grown from physical vapor transport (PVT). This growth method yields orange crystals with orthorhombic symmetry, space group *Cmca*. We notice that the polymorph of the crystals grown with this method coincides[2] with that obtained

[2]We used the standard settings of the International Tables for Crystallography. The transformation to *Bbam* (*Cmca* $\rightarrow$ *Bbam*) is: $b \rightarrow a$, $c \rightarrow b$, $a \rightarrow c$. For the crystal orientation in the electronic measurements [2,3], the *Bbam* setting was used.

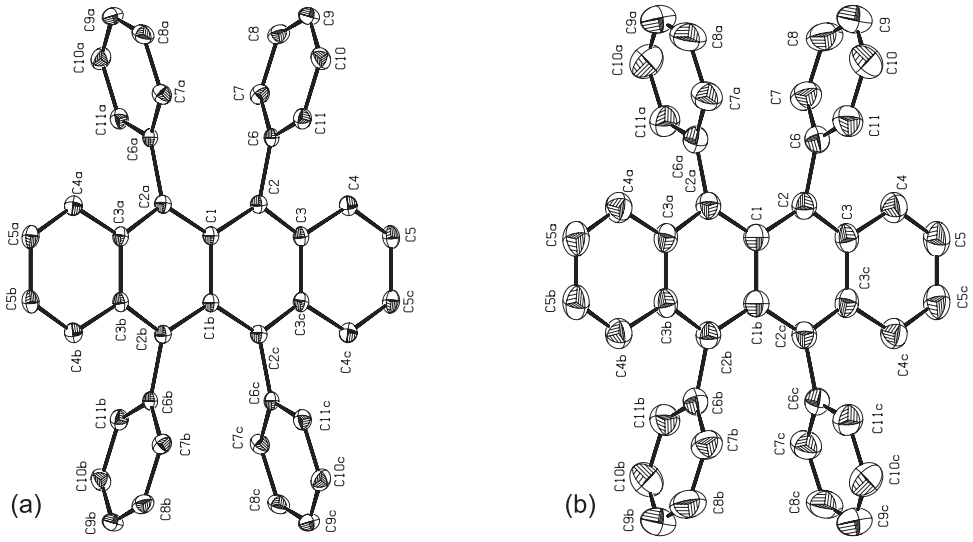

Figure 6.2: Perspective ORTEP drawing of the rubrene molecule illustrating the configuration and the adopted labelling scheme for the non-hydrogen atoms at 100 K (a), and room temperature (b). Displacement ellipsoids for non-H are represented at the 50% probability level.

.

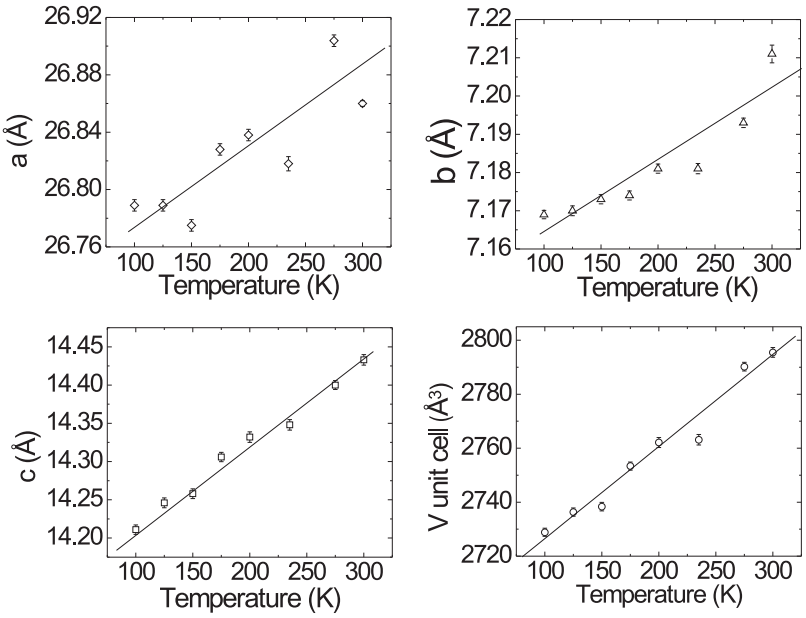

Figure 6.3: Lattice parameters a, b and c, and unit cell volume V versus temperature for rubrene single crystals. The lines are guides for the eyes.

for the crystals grown in sealed ampoules by Bulgarovskaya *et al.* [10].

The molecule presents $2/m$ symmetry, with the asymmetric unit consisting of one quarter of a rubrene molecule. A twofold axis is located along the $C1 - C1b$ bond. There is a mirror plane perpendicular to the planar tetracene fragment of the molecule, through the inversion center positioned in the middle of the $C1-C1b$ bond. The adopted labelling scheme and the molecular geometry are illustrated in the ORTEP drawings of Figure 6.2(a, b). The plots show graphical representations of the atomic positions and their anisotropic displacement ellipsoids at the minimum and maximum temperatures investigated in this study (T=100 K, and room temperature). These images provide a visual description of the vibrational motions of each atom around its equilibrium position.

The crystal structure determination reveals a 2.157% volume thermal expansion of the crystal between 100 K and 300 K, in agreement with typical values measured in organic crystals. The thermal expansion is anisotropic for the three crystallographic directions ($\Delta a = 0.410\%$, $\Delta b = 0.320\%$, $\Delta c = 1.562\%$) and oc-

curs predominantly along the weakest bonding c-axis (see Fig. 6.3). The lattice parameters together with other crystallographic parameters for all eight temperature structures investigated in this study can be found in the Appendix B of the thesis.

6.5 Relation between molecular stacking and electronic mobility

We relate the behavior of electronic mobility versus temperature with structural changes. Electronic measurements performed on rubrene single crystals show that the field effect mobility increases with decreasing temperature down to 175 K, consistent with band-like behavior [2, 3] (the results differ slightly between groups). Below 175 K the mobility drops precipitously. The dramatic decrease in the field-effect mobility can be a consequence of a structural phase transition in the material. Our diffraction experiments show that the crystallographic symmetry does not change when passing in this temperature interval. It can also be observed from Figure 6.3 that the unit cell volume and unit cell parameters are continuous with temperature within our resolution. Also, the evolution of the fractional coordinates of the Carbon atoms do not signal the presence of a phase transition. However, differential scanning calorimetry (DSC) performed on the crystals exhibit the signature of a phase transition around $T = 175$ K (see Fig. 6.4). It is likely that there is a phase transition at this temperature, but it is not observable from our X-ray diffraction experiments.

We use the model proposed by da Silva Filho *et al.* [13] to explain the changes in electronic properties as a response to the structural changes in the crystal. They associate the intrinsic transport properties of rubrene single crystals with the electronic coupling between adjacent molecules. The measure for this interaction is the interchain transfer integral, t, which varies with molecular packing. The electronic coupling is maximal if the molecules are perfect cofacial in the crystal, oscillates when the molecular displacement increases (with positive and negative values) and becomes zero at large shifts. This translates to the direct influence of the molecular stacking on the electronic properties.

It can bee seen in Figure 6.5 that the molecules are not perfectly cofacial, but they are shifted with respect to each other. We define the *molecular displacement* d that quantifies the shift between two molecules. From the calculations of Silva Filho *et al.* it is obvious that the molecular displacement, d, is the relevant parameter, relating the crystal structure with the electronic mobility, similar to

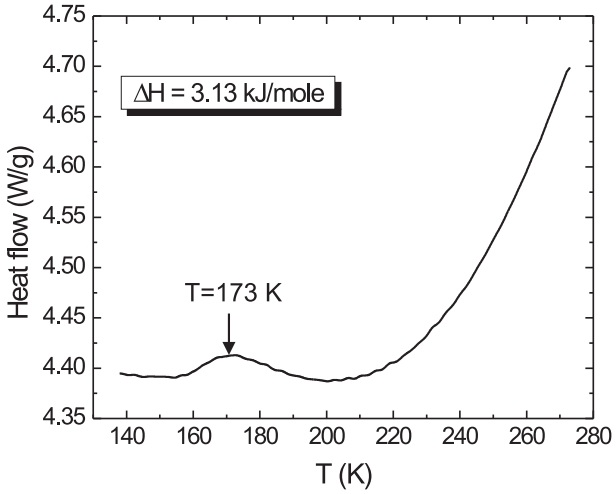

Figure 6.4: Differential Scanning Calorimetry of crushed rubrene single-crystals. The measurement has been carried out in N_2 atmosphere. The enthalpy associated with the transition is 3.13 kJ/mole. The arrow indicates the position or the peak.

the model proposed by Mattheus *et al.* [14]. This parameter is complementary to molecular overlap and given by the orientation of the tetracene backbone with respect to the b - crystallographic direction.

In order to calculate the value of molecular displacement at each temperature, we show the projection of two rubrene molecules on the b-c plane (see Fig. 6.6). From geometrical considerations, the value of the molecular displacement (d) is given by: (Eq. 6.1):

$$d = r + q \tag{6.1}$$

where r represents half of the length of the rubrene molecule, and q the distance from the extremity of the one molecule to the perpendicular taken from the middle of the molecule to the long axis of the other one. The simplified expression for d at each temperature is:

$$d = b \cdot \cos\Theta \tag{6.2}$$

where b is the value of the unit cell parameter (Fig. 6.3) and Θ is the angle that the linear part of the molecule makes with this axis.

The maximum deviation from planarity in the tetracene backbone of the molecule corresponds to C2 and is 0.0714(11) Å at 100 K and 0.0731(14) Å

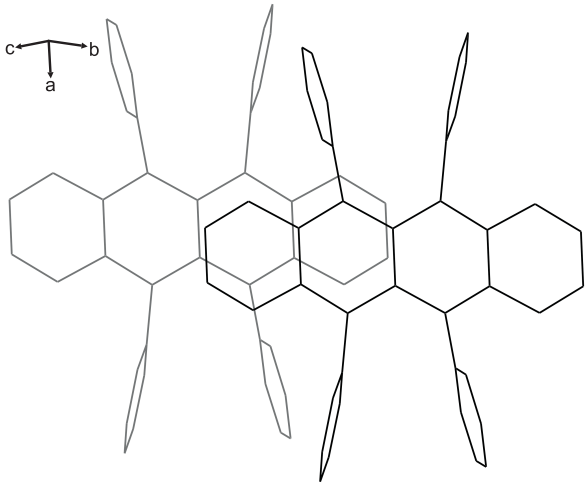

Figure 6.5: Schematic representation of two rubrene molecules in the crystal. The π- stacking distance is similar to van der Waals distance. The molecules are shifted with respect to each other along the tetracene backbone.

.

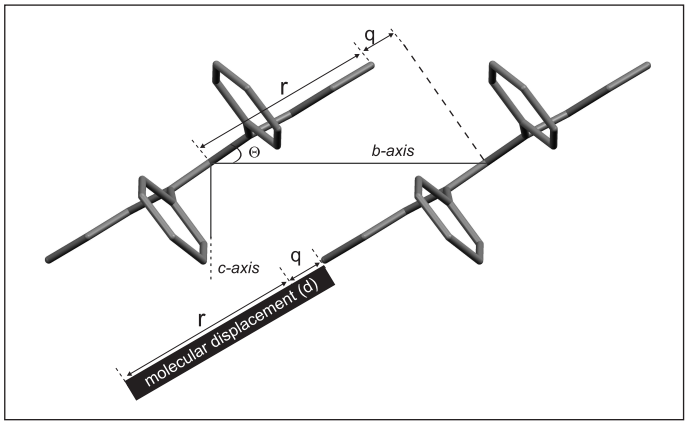

Figure 6.6: Arrangement of the rubrene molecules in the unit cell: view along the [100] axis. The drawing includes schematic representation of the parameters (r, q) used in the calculation of the molecular displacement (d). Unit cell b and c axis are also indicated. Θ is the angle between the long axis of the molecule and b-axis.

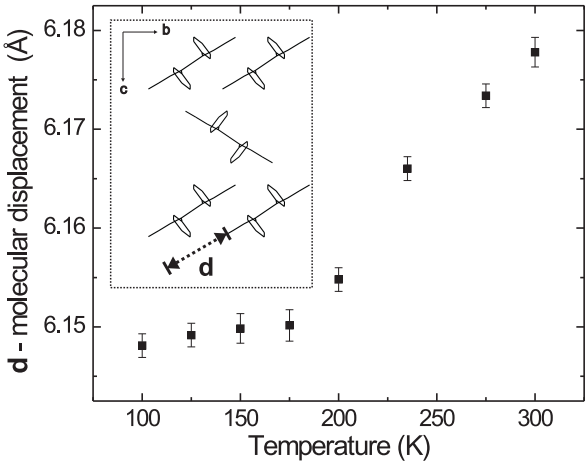

Figure 6.7: Evolution of the molecular displacement along the long axis of the rubrene molecule with temperature. The inset represents rubrene molecular packing viewed along the [100] direction, and defines the length d of the molecular displacement.

at room temperature. The interplanar separation between two adjacent parallel molecules, along the π-stack, increases from 3.654(3) Å to 3.715(3) Å between 100 K and 300 K. This length is slightly larger than the typical van der Waals interaction distance in a $C-C$ π-stack [15].

The molecules slide with respect to each other along their long axis when the temperature is modified. Figure 6.7 shows the temperature dependence of the molecular displacement, d along the long axis of the molecule in rubrene single crystal. The value of the shift increases between 100 K and 300 K (Fig. 6.7). The changes of d with temperature are dominated by changes in the lattice parameter b (see Fig. 6.3). However, it can be seen from Figure 6.3 and Figure 6.8, that the temperature dependence of b and $cos(\Theta)$ individually do not present any discontinuity or change of slope at $T = 175$ K. In spite of the fact that a different picture is suggested by their combination in the molecular displacement (see Eq. 6.2), we cannot assign this to a crystallographic phase transition.

The variations in molecular displacement induce changes in the transfer integral (t), and determine the electronic mobility (see Figure 4, da Silva Filho

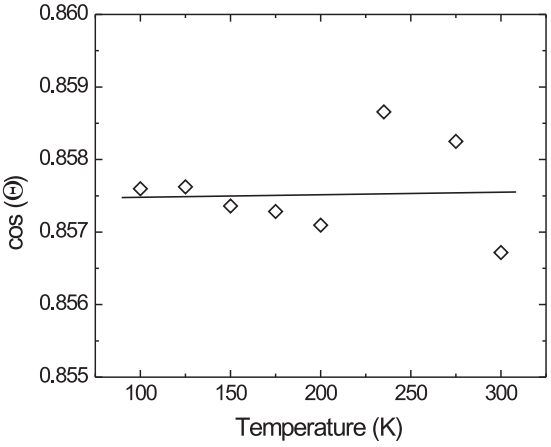

Figure 6.8: Variation of the angle Θ between the tetracene backbone of rubrene molecule and the b crystallographic axis.

et al., [13]). The molecular displacement has a large value due to the effect of the interactions between phenyl side groups of neighboring molecules. They are arranged two by two, on different sides of the planar tetracene part of rubrene and the position is restricted by the inversion center. Their torsion with respect to the acene linear part ranges from 80.30(5)° at 100 K to 80.88(7)° at room temperature. The phenyl rings positioned on the same part of the molecule make a dihedral angle of 25.32(6)° at 100 K and 25.14(10)° at 300 K. The connection between the phenyl rings and the tetracene fragment is the $C_2 - C_6$ bond. At 100 K this bond makes an angle of 12.57(8)° with the tetracene fragment of the molecule and 6.13(9)° with the phenyl-plane. The corresponding angles at 300 K are 12.74(9)° and 6.00(10)°, respectively.

6.6 Conclusions

We conclude that rubrene single crystals grown from physical vapor transport in ambient pressure exhibit an orthorhombic symmetry. We find evidence for a phase transition from DSC measurements, but see no evidence for a structural phase transition in the diffraction experiments. Further investigations concerning the mechanism that drives the dramatic changes in electronic mobility at $T = 175$ K in rubrene are required.

References

[1] V. C. Sundar, J. Zaumseil, V. Podzorov, E. Menard, R. L. Willett, T. Someya, M. E. Gershenson, and J. A. Rogers, Science **303**, 1644 (2004)

[2] R. W. I. de Boer, M. E. Gershenson, A. F. Morpurgo, and V. Podzorov, Phys. Stat. Sol. A **201**, 1302 (2004)

[3] V. Podzorov, E. Menard, A. Borissov, V. Kiryukhin, J. A. Rogers, and M. E. Gershenson, Phys. Rev. Lett. **93**, 086602 (2004)

[4] V. Y. Butko, J. C. Lashley, and A. P. Ramirez, Phys. Rev. B **72**, 081312 (2005)

[5] T. Oyamada, H. Uchiuzou, S. Akiyama, Y. Oku, N. Shimoji, K. Matsushige, H. Sasabe, and C. Adachi, J. Appl. Phys. **98**, 074506 (2005)

[6] C. N. Li, C. Y. Kwong, A. B. Djurisic, P. T. Lai, P. C. Chui, W. K. Chan, and S. Y. Liu, Thin Solid Films **477**, 57 (2005)

[7] W. H. Taylor, Z. Kristallogr. **93**, 151 (1936).

[8] S. A. Akopyan, R. L. Avoyan, and Yu. T. Struchkov, Z. Strukt. Khim. **3**, 602 (1962)

[9] D. E. Henn, and W. G. Williams, J. Appl. Cryst. **4**, 256 (1971)

[10] I. Bulgarovskaya, V. Vozzhennikov, S. Aleksandrov, and V. Belsky, Latv. PSR Zinat. Akad. Vestis, Fiz. Teh. Zinat. Ser. **4**, 53 (1983)

[11] A. Laudise, C. Kloc, P. Simpkins, and T. Siegrist, J. Cryst. Growth **187**, 449 (1998)

[12] O. D. Jurchescu, J. Baas, and T. T. M. Palstra, Appl. Phys. Lett **84**, 3061 (2004)

[13] D. A. da Silva Filho, E. G. Kim, and J.-L. Brédas, Adv. Mat. **17**, 1072 (2005)

[14] C. C. Mattheus, G. A. de Wijs, R. A. de Groot, and T. T. M. Palstra, J. Am. Chem. Soc. **125**, 6323 (2003)

[15] A. Bondi, J. Phys. Chem. **68**, 441 (1964)